Neutrino Fits

Thomas Schwetz

Institut für Kernphysik, Karlsruher Institut für Technologie (KIT), D-76021 Karlsruhe, Germany

In the first part of the talk I present the results of a global fit to neutrino oscillation data focusing on the standard three-flavour scenario. The determination of all oscillation parameters is presented and I comment on the status of the CP phase, for which current data indicates a preference of the range $\pi \lesssim \delta_{\rm CP} \lesssim 2\pi$ over $0 \lesssim \delta_{\rm CP} \lesssim \pi$. Furthermore I discuss the issue of normal versus inverted mass ordering which are degenerate at the 1σ level in our global fit. I comment also on the possibility to use cosmological data to disfavour the inverted mass ordering, arguing that using current data this is not significant. In the last part I discuss the possible presence of non-standard neutrino interactions. If new interaction of similar size as weak interactions are allowed, the so-called LMA-dark solution appears. It corresponds to an exact degeneracy in the neutrino evolution, which leads to a generalized mass ordering degeneracy and makes the determination of the neutrino mass ordering with oscillation experiments impossible. The only way to break this degeneracy is by using non-oscillation observables, for instance neutrino scattering data at low energy.

1 Three-flavour oscillations

Thanks to remarkable results of many neutrino oscillation experiments we have now a rather clear picture of the three-flavour leptonic mixing matrix and the ordering of the neutrino mass states has been narrowed down to two possibilities, called normal and inverted orderings. The present status of the standard 3-flavour oscillation scenario is summarized in Fig. 1, where we show the results of a global fit in terms of the two mass squared-differences, the three mixing angles, and the complex phase relevant for neutrino oscillations. Those results correspond to NuFit-3.0 [1], where a precise definition of the parameters as well as a description of the used data can be found. Tables with χ^2 data are available at the NuFit website [2], where also future updates will be published.

Defining the 3σ relative precision of a parameter by $2(x^{\rm up} - x^{\rm low})/(x^{\rm up} + x^{\rm low})$, where $x^{\rm up}$ ($x^{\rm low}$) is the upper (lower) bound on a parameter x at the 3σ level, we read 3σ relative precision of 14% (θ_{12}), 32% (θ_{23}), 11% (θ_{13}), 14% (Δm^2_{21}) and 9% ($|\Delta m^2_{3\ell}|$) for the various oscillation

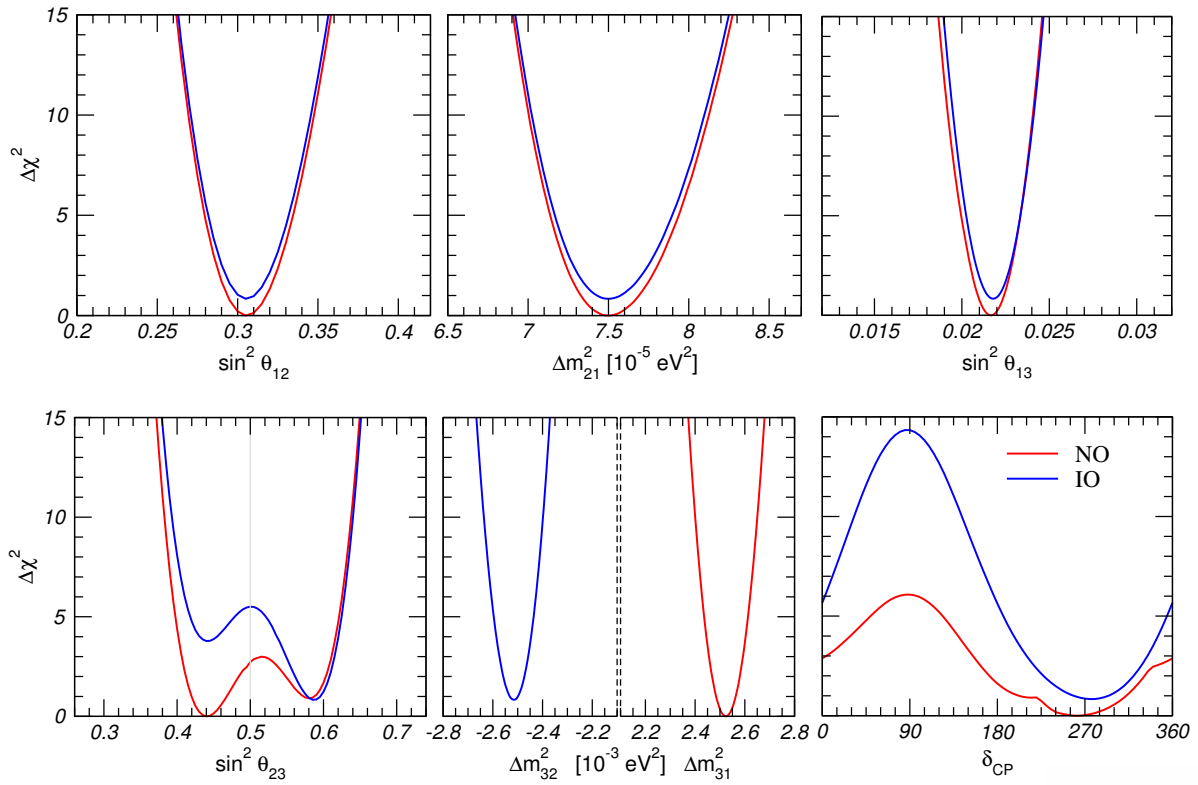

Figure 1 – Global fit results from NuFit-3.0 [1,2]. We show the 1-dimensional $\Delta\chi^2$ projections for the various parameters on the horizontal axes. Red (blue) curves are for the normal (inverted) mass ordering.

parameters. We observe that for θ_{23} the uncertainty is still relatively large and there is the ambiguity of first octant/maximal mixing/second octant.

1.1 Leptonic CP violation

A nontrivial value of the complex phase in the lepton mixing matrix leads to differences of the vacuum transition probabilities for neutrinos and antineutrinos. The effect is proportional to the Jarlskog invariant which gives a convention-independent measure of CP violation [3]:

$$\Im\left[U_{\alpha i}U^*_{\alpha j}U^*_{\beta i}U_{\beta j}\right] \equiv J^{\rm max}_{\rm CP}\sin\delta = \cos\theta_{12}\sin\theta_{12}\cos\theta_{23}\sin\theta_{23}\cos^2\theta_{13}\sin\theta_{13}\sin\delta \qquad (1)$$

where we have used the standard parametrization of the mixing matrix in terms of angles and the Dirac complex phase. Thus the determination of the mixing angles yields at present a maximum allowed CP violation of

$$J^{\rm max}_{\rm CP} = 0.0329 \pm 0.0007\,(^{+0.0021}_{-0.0024}) \qquad (2)$$

at 1σ (3σ) for both orderings. Comparing this result with the size of the Jarlskog invariant in the quark sector [4], $J^{\rm quarks}_{\rm CP} = (3.04^{+0.21}_{-0.20}) \times 10^{-5}$, we observe that leptonic CP violation can be potentially 3 orders of magnitude larger than for quarks.

As visible in the lower right panel of Fig. 1, current data favours values of $\pi \lesssim \delta_{\rm CP} \lesssim 2\pi$ compared to the range $0 \lesssim \delta_{\rm CP} \lesssim \pi$. The best fit value is at $\delta_{\rm CP} \approx 3\pi/2$, CP conservation (i.e., $\delta_{\rm CP} = 0$ or π) is allowed at 70% CL for normal ordering and 97% CL for inverted ordering, and $\delta_{\rm CP} \approx \pi/2$ is disfavoured with $\Delta\chi^2 \approx 6\,(14)$ for normal (inverted) ordering. The preference for non-zero $\delta_{\rm CP}$ implies a best fit value $J^{\rm best}_{\rm CP} = -0.033$. Fig. 2 shows that there is significant correlation between $\delta_{\rm CP}$ and the mixing angle θ_{23}.

The current indication for $\delta_{\rm CP} \approx 3\pi/2$ is driven mostly by T2K data [5]. It happens that both neutrino and antineutrino event numbers feature a statistical fluctuation in the "right"

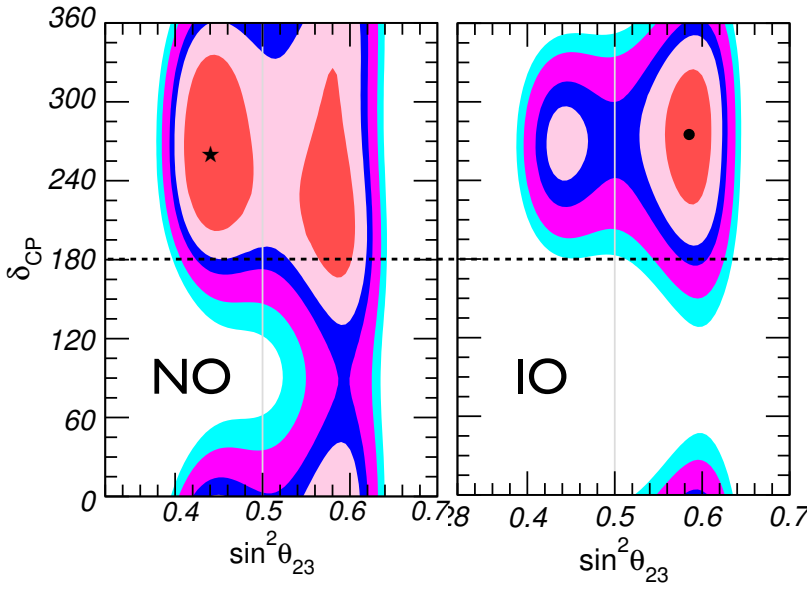

Figure 2 – Global fit results from NuFit-3.0 [1,2] projected onto the plane of δ_{CP} and $\sin^2\theta_{23}$ for normal (left) and inverted (right) mass ordering. The different contours correspond to 1σ, 90%, 2σ, 99%, 3σ CL (2 dof). Regions for IO are shown with respect to the global best fit point, which happens for NO and is indicated by the star.

$\delta_{CP,true}$	NO/2nd Oct.	IO/1st Oct.	IO/2nd Oct.
0°	62%	91%	28%
180°	56%	89%	32%
270°	70%	83%	27%
Gaussian	72%	94%	46%

Table 1: CL for the rejection of various combinations of mass ordering and θ_{23} octant with respect to the global best fit (which happens for NO and 1st octant). We quote the CL of the local minima for each ordering/octant combination, assuming three example values for the true value of δ_{CP} as well as for the Gaussian approximation (last row). Resuts taken from [1].

direction. While fully consistent within statistical uncertainties, it may happen, however, that the significance for δ_{CP} will grow slower than the square-root of the exposure.

1.2 Neutrino mass ordering

The discrimination of normal ordering (NO) versus inverted ordering (IO) is one of the major open tasks for neutrino oscillation experiments. We observe from Fig. 1 that the fits of the two orderings are essentially degenerate for present data, with $\Delta\chi^2 \approx 1$. As visible in the lower left panel, the sensitivity to the mass ordering is entangled with the octant of θ_{23}. In Tab. 1 we show the CL at which a certain combination of mass ordering and θ_{23} octant can be excluded with respect to the global minimum, which occurs for NO and the 1st θ_{23} octant. The CL has been determined by performing a Monte Carlo simulation to obtain the distribution of the $\Delta\chi^2$ statistic numerically [1], see also [6]. We observe that the CL of the second octant for NO shows relatively large deviations from Gaussianity and dependence on the true value of δ_{CP}. In any case, the sensitivity is very low and the 2nd octant can be reject at most at 70% CL (1σ) for all values of δ_{CP}. The first octant for IO can be excluded at between 83% and 91% CL, depending on δ_{CP}. The exclusion of the IO/2nd octant case corresponds also to the exclusion of the IO, since at that point the confidence interval in IO would vanish. Also in this case we observe deviations from the Gaussian approximation and the CL of at best 32% is clearly less than 1σ, showing that the considered data set has essentially no sensitivity to the mass ordering.

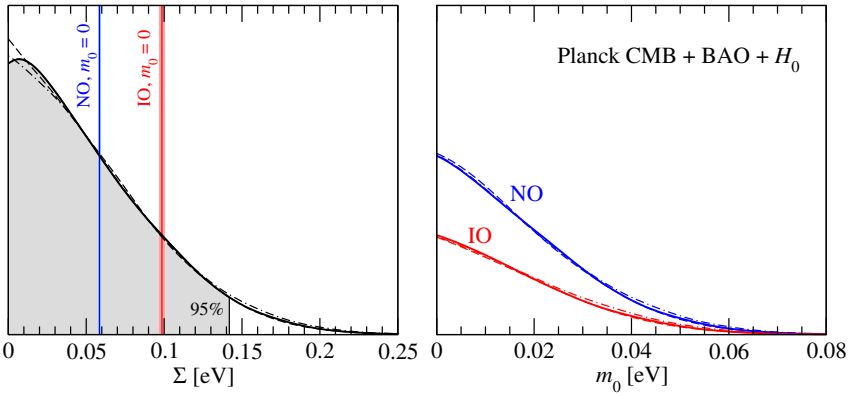

Figure 3 – Posterior likelihood function from current data (Planck+BAO+H_0). The left panel shows the posterior likelihood function for Σ, where we indicate the predicted values for NO and IO in the case of $m_0 = 0$; the width of the lines corresponds to $\pm 2\sigma$ uncertainty due to current oscillation data. The gray shaded region indicates the one-sided upper bound on Σ at 95% CL (flat prior in Σ). The right panel shows the posterior likelihood as a function of the lightest neutrino mass, m_0, for NO and IO with appropriate relative normalization. Results from Ref. [9].

We note that the SuperKamiokande collaboration reports [7] a preliminary hint from atmospheric neutrino data in favour of the NO with $\Delta\chi^2 \approx 4.3$. Unfortunately with the public available information it is not possible to reproduce this result outside the collaboration and therefore these data cannot be included in the global fit.

Some information on the mass ordering can be obtained also from observables sensitive to the absolute neutrino mass. Here we briefly mention the information coming from cosmology, which is sensitive to the sum of the neutrino masses, Σ. For a vanishing lightest neutrino mass ($m_0 = 0$), the predictions for the sum are (1σ uncertainties)

$$\Sigma = \begin{cases} 58.5 \pm 0.48\,\text{meV} & \text{(NO)} \\ 98.6 \pm 0.85\,\text{meV} & \text{(IO)} \end{cases} \qquad (m_0 = 0)\,. \tag{3}$$

Hence, if cosmological observations provide a determination of Σ significantly below 0.098 eV, the inverted mass ordering would be disfavoured.[a] Recent data from Planck CMB observations combined with baryonic acoustic oscillations (BAO) and other observations lead to the bound $\Sigma < 0.23$ eV at 95% CL (PlanckTT + lowP + lensing + BAO + JLA + H_0), see [8] for details. Depending on the used data and variations in the analysis, different authors obtain upper bounds from current data approaching the "critical" value of 0.1 eV. In Ref. [9] we have adopted a particular combination of data which leads to an upper bound of 0.14 eV at 95% CL.

As illustrated in the left panel of Fig. 3, we see that both orderings are well compatible with such a bound. In Ref. [9] we propose a statistical method to quantify this statement, based on Bayesian model selection. In this framework, the posterior odds of NO versus IO are obtained as the ratio of the area under the likelihood curves shown in the right panel of Fig. 3, assuming a flat prior on the lightest neutrino mass. We find that present data leads to posterior odds of about 3:2 in favour of NO. In order to obtain a significant rejection of IO from cosmology, a sensitivity to Σ better than 0.02 eV (1σ) is needed. Such a sensitivity could be achieved by 2 years of data from the EUCLID project, see Ref. [9] for a simulation. Comparing this sensitivity with the values given in Eq. (3), we see that with such a sensitivity a 3σ evidence for a non-zero Σ will be obtained even for NO with vanishing lightest neutrino mass.

2 Beyond three-flavour: non-standard neutrino interactions

The three-flavour neutrino paradigm is well established and most new-physics scenarios lead to small perturbation of the standard picture. One example for this statement are light sterile

[a] Note that cosmology can only exclude IO but cannot favour IO over NO.

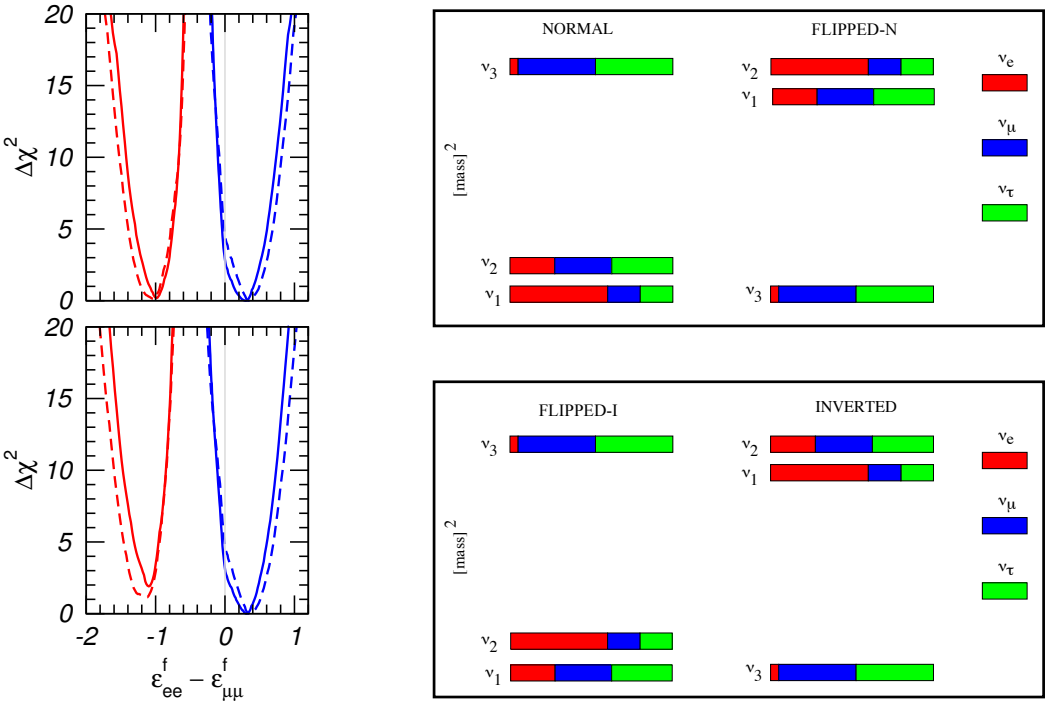

Figure 4 – On the left we show the $\Delta\chi^2$ as a function of $\epsilon^u_{ee} - \epsilon^u_{\mu\mu}$ (upper panel) and $\epsilon^d_{ee} - \epsilon^d_{\mu\mu}$ (lower panel). The blue curves correspond to $\theta_{12} < 45^\circ$ and the red curves to $\theta_{12} > 45^\circ$ (the so-called LMA-dark solution), taken from Ref. [13]. On the right we show the four possible orderings of the neutrino mass states, corresponding to the generalized neutrino mass ordering degeneracy [15].

neutrinos [10]. Here we comment on an exception to the above statement, a particular new-physics scenario where actually order-one modifications of standard physics are still allowed by data, namely so-called non-standard neutrino interactions (NSI).

We consider the presence of neutral-current (NC) NSI in the form of dimension-6 four-fermion operators, for recent reviews see e.g. [11]. NSI are described by the Lagrangian

$$\mathcal{L}_{\rm NSI} = -2\sqrt{2} G_F \epsilon^f_{\alpha\beta} (\overline{\nu}_{\alpha L} \gamma^\mu \nu_{\beta L})(\overline{f} \gamma_\mu f)\,, \tag{4}$$

where, $\alpha, \beta = e, \mu, \tau$, and f denotes a fermion present in the background medium. The parameter $\epsilon^f_{\alpha\beta}$ parametrizes the strength of the new interaction with respect to the Fermi constant G_F. Hermiticity requires that $\epsilon^f_{\alpha\beta} = (\epsilon^f_{\beta\alpha})^*$. Note that we restrict to vector interactions, since we are interested in the contribution of NSI to the effective matter potential [12].

A comprehensive study of the allowed values for NSI has been preformed in Ref. [13]. Typically the values of $\epsilon^f_{\alpha\beta}$ have to be less than few percent, with two exceptions: (i) for $\epsilon^f_{e\tau}$ the limits are around 0.14 (90% CL), and (ii) for the combination $\epsilon^u_{ee} - \epsilon^u_{\mu\mu}$ there are actually two degenerate solutions. The best fit solution corresponds approximately to $\epsilon^u_{ee} - \epsilon^u_{\mu\mu} \approx 0.3$ (see Fig. 4, left, blue curves). This relatively large value is driven by a 2σ tension in the solar neutrino spectrum measured at SuperKamiokande and SNO. In the presence of NSI of this size, the low-energy part of the spectrum can be better fitted to the data, which currently do not yet follow the predicted up-turn of the standard MSW solution.

However, in addition, there is a second quasi-degenerate solution (Fig. 4, left, red curves) with $\epsilon^u_{ee} - \epsilon^u_{\mu\mu} \approx -1$ and the solar mixing angle in the second octant, $\theta_{12} > 45^\circ$, the so-called LMA-dark solution [14]. As discussed in [15] (see also [13,16]) this degeneracy is a manifestation of a general symmetry: as a consequence of the CPT symmetry, neutrino evolution is invariant if the corresponding Hamiltonian is transformed as $H \to -H^*$. This transformation can be realised

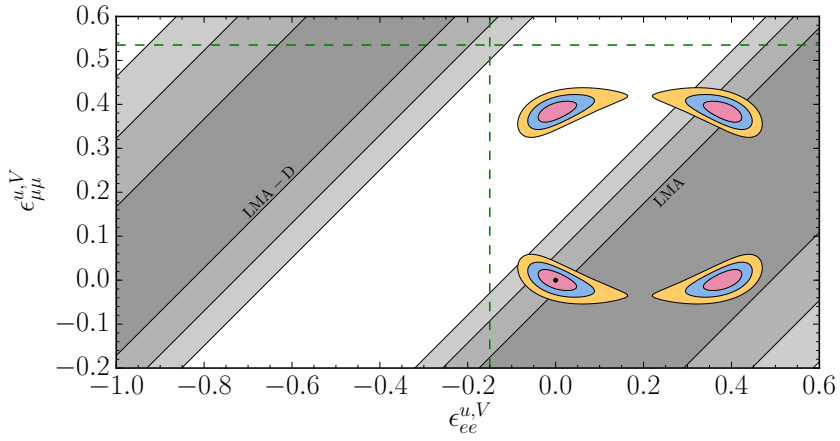

Figure 5 – Allowed regions (sensitivity) in the plane of ϵ_{ee}^{u} and $\epsilon_{\mu\mu}^{u}$ from the COHERENT experiment [19] under the assumption of no NSI in the data, overlayed with the presently allowed regions from the global oscillation analysis. The two diagonal shaded bands correspond to the LMA and LMA-dark regions as indicated, at 1, 2, 3σ. The dashed lines indicate the values of NSI parameters for which COHERENT would not be able to resolve the LMA-dark degeneracy. Plot from Ref. [17].

by changing the oscillation parameters as

$$\begin{aligned} &\Delta m^2_{31} \to -\Delta m^2_{31} + \Delta m^2_{21} = -\Delta m^2_{32}\,, \\ &\sin\theta_{12} \leftrightarrow \cos\theta_{12}\,, \\ &\delta \to \pi - \delta\,, \end{aligned} \tag{5}$$

and simultaneously transforming the NSI parameters as

$$\begin{aligned} &(\epsilon_{ee} - \epsilon_{\mu\mu}) \to -(\epsilon_{ee} - \epsilon_{\mu\mu}) - 2\,, \\ &(\epsilon_{\tau\tau} - \epsilon_{\mu\mu}) \to -(\epsilon_{\tau\tau} - \epsilon_{\mu\mu})\,, \\ &\epsilon_{\alpha\beta} \to -\epsilon^*_{\alpha\beta} \qquad (\alpha \neq \beta)\,, \end{aligned} \tag{6}$$

In Eq. (5), δ is the leptonic Dirac CP phase, and we are using here the parameterization conventions from Ref. [15]. In Eq. (6) we take into account explicitly that oscillation data are only sensitive to differences in the diagonal elements of the Hamiltonian. Eq. (5) shows that this degeneracy implies a change in the octant of θ_{12}, i.e., the LMA-dark solution, as well as a change in the neutrino mass ordering, i.e., the sign of Δm^2_{31}. For that reason it has been called "generalized mass ordering degeneracy" in Ref. [15].

The corresponding mass spectra are illustrated in Fig. 4, right. The spectra based on large NSI feature "flipped" solar mass states (corresponding to $\theta_{12} > 45°$). Since the degeneracy is an exact symmetry of the Hamiltonian for any arbitrary matter profile, the flipped spectra are indistinguishable from the standard ones by any combination of oscillation experiments. Hence, if one allows for the presence of large NSI, the determination of the mass ordering with oscillation experiments becomes impossible. The only way to resolve this degeneracy is by using non-oscillation observables, for instance experiments measuring the neutrino–quark neutral-current scattering cross section [15]. In order to fully exclude the degenerate solution, data on the ν_e as well as ν_μ cross section are required. A combined analysis of scattering and oscillation data has been performed in Ref. [17].

In generic models of new physics NSI parameters are expected to be small. However, examples of viable gauge models leading to $\epsilon^{u,d}_{\alpha\beta} \sim \mathcal{O}(1)$ can be found in [18]. Typically such large NSI can be achieved by assuming light mediator particles. This has important consequences for scattering experiments, since if the momentum transfer in the experiment is much larger than the mediator mass, the effect will be suppressed. Hence, the preferred configuration to constrain

NSI are low-energy scattering experiments, such as for instance coherent neutrino–nucleon scattering experiments. In Ref. [17] we have shown that such an experiment performed at a stopped pion source will either rule out the NSI-based degeneracy or discover non-zero NSI, see Fig. 5.

Acknowledgments. The author has received funding from the European Unions Horizon 2020 research and innovation programme under the Marie Sklodowska-Curie grant agreement No 674896 (Elusives).

References

1. I. Esteban, M. C. Gonzalez-Garcia, M. Maltoni, I. Martínez-Soler and T. Schwetz, "Updated Fit to Three Neutrino Mixing: Exploring the Accelerator-Reactor Complementarity," JHEP **1701** (2017) 087 [arXiv:1611.01514].
2. NuFit website: `www.nu-fit.org`
3. C. Jarlskog, "Commutator of the Quark Mass Matrices in the Standard Electroweak Model and a Measure of Maximal CP Violation," Phys. Rev. Lett. **55** (1985) 1039.
4. C. Patrignani *et al.* [Particle Data Group], "Review of Particle Physics," Chin. Phys. C **40** (2016) no.10, 100001.
5. K. Abe *et al.* [T2K Collaboration], "Combined Analysis of Neutrino and Antineutrino Oscillations at T2K," Phys. Rev. Lett. **118** (2017) no.15, 151801 [arXiv:1701.00432].
6. J. Elevant and T. Schwetz, "On the Determination of the Leptonic CP Phase," JHEP **1509** (2015) 016 [arXiv:1506.07685].
7. SuperKamiokande Coll., talk by J. Kameda, NuFact 2016, Vietnam `http://vietnam.in2p3.fr/2016/nufact/index.html`
8. P. A. R. Ade *et al.* [Planck Collaboration], "Planck 2015 results. XIII. Cosmological parameters," Astron. Astrophys. **594** (2016) A13 [arXiv:1502.01589].
9. S. Hannestad and T. Schwetz, "Cosmology and the Neutrino Mass Ordering," JCAP **1611** (2016) no.11, 035 [arXiv:1606.04691].
10. C. Giunti, these proceedings.
11. O. G. Miranda and H. Nunokawa, "Non Standard Neutrino Interactions: Current Status and Future Prospects," New J. Phys. **17** (2015) no.9, 095002 [arXiv:1505.06254]; T. Ohlsson, "Status of Non-Standard Neutrino Interactions," Rept. Prog. Phys. **76** (2013) 044201 [arXiv:1209.2710].
12. L. Wolfenstein, "Neutrino Oscillations in Matter," Phys. Rev. D **17** (1978) 2369.
13. M. C. Gonzalez-Garcia and M. Maltoni, "Determination of Matter Potential from Global Analysis of Neutrino Oscillation Data," JHEP **1309** (2013) 152 [arXiv:1307.3092].
14. O. G. Miranda, M. A. Tortola and J. W. F. Valle, "Are Solar Neutrino Oscillations Robust?," JHEP **0610** (2006) 008 [hep-ph/0406280].
15. P. Coloma and T. Schwetz, "Generalized Mass Ordering Degeneracy in Neutrino Oscillation Experiments," Phys. Rev. D **94** (2016) no.5, 055005 [arXiv:1604.05772].
16. P. Bakhti and Y. Farzan, "Shedding Light on Lma-Dark Solar Neutrino Solution by Medium Baseline Reactor Experiments: Juno and Reno-50," JHEP **1407** (2014) 064 [arXiv:1403.0744].
17. P. Coloma, P. B. Denton, M. C. Gonzalez-Garcia, M. Maltoni and T. Schwetz, "Curtailing the Dark Side in Non-Standard Neutrino Interactions," JHEP **1704** (2017) 116 [arXiv:1701.04828].
18. Y. Farzan, "A Model for Large Non-Standard Interactions of Neutrinos Leading to the Lma-Dark Solution," Phys. Lett. B **748** (2015) 311 [arXiv:1505.06906]; Y. Farzan and J. Heeck, "Neutrinophilic Nonstandard Interactions," Phys. Rev. D **94** (2016) no.5, 053010 [arXiv:1607.07616].
19. D. Akimov *et al.* [COHERENT Collaboration], "The Coherent Experiment at the Spallation Neutron Source," arXiv:1509.08702 [physics.ins-det].